

Performance Analysis of Multicode OCDM Networks Supporting Elastic Transmission With QoS Differentiation

Ahmed E. A. Farghal, Hossam M. H. Shalaby, *Senior Member, IEEE*, Kazutoshi Kato, *Senior Member, IEEE*, and Ramesh K. Pokharel, *Member, IEEE*

Abstract—A multicode optical code-division multiplexing (OCDM) is proposed to support the dynamic changes in the requested traffic demand in OCDM networks by adapting the number of allocated codes according to the requested transmission rate. In order to support time-variant data rates and multiservice transmissions; a multicode variable-weight 2D one-coincidence frequency hopping code/optical orthogonal code (OCFHC/OOC) is employed as the signature code in the proposed system. Two multicode assignment methods, namely, random multicode assignment (RMA) policy and uniform multicode assignment (UMA) policy, are presented. For each code assignment method, we derive the probability density function (pdf) of the number of active codes in each wavelength group. The bit error probability (BEP), the probability of degradation, and the blocking probability are derived as network performance key parameters. The proposed system has a simplified routing and code assignment process with a lower blocking probability. Our numerical results indicate that the network teletraffic capacity and blocking probability can be improved significantly using UMA policy and call admission control.

Index Terms—Optical code-division multiplexing (OCDM), multicode, blocking probability, QoS, spectral efficiency.

I. INTRODUCTION

FUTURE optical networks are expected to support a large number of users with diverse data rates and quality-of-service (QoS) demands in a flexible manner. Traditional wavelength-division multiplexing (WDM) networks suffer from rigid and coarse granularity (i.e., 50 or 100 GHz ITU-T WDM grid), which results in inefficient capacity usage (due to bandwidth over-provisioning for lower data rate traffic) and

inflexible support of diverse bandwidth demands [1], [2]. On the other hand, optical time-division multiplexing (TDM) networks have stringent *end-to-end* synchronization requirements along the optical path and only a fixed number of time-slots can be allocated in a single wavelength [3].

Optical code-division multiplexing (OCDM) can provide flexible, heterogeneous, asynchronous multiple bit-rate transmissions with finer-granularity capacity at sub-wavelength level to connections with enhanced security and network scalability [3]–[6]. In addition, OCDM can provide QoS differentiation at the physical layer level. Moreover, no channel control mechanism is needed to assign bandwidth or avoid collisions in OCDM. Further, optical code generation, processing, and decoding is performed entirely in the optical domain.

In this work, we propose and analyze a multicode OCDM network where a service request is allocated a number of codes in proportion to the desired data rate. Two-dimensional (2D) one-coincidence frequency-hopping code/optical orthogonal codes (OCFHC/OOCs) [7] are used as the signature sequences in the proposed network. The proposed multicode OCDM network can support the dynamic changes in the requested rate by means of allocating/de-allocating encoders/decoders to the existing connections. We also employ different code weights for different classes to provide QoS differentiation in terms of bit error probability (BEP). The proposed multicode OCDM is compatible with the current technology of conventional WDM networks operating on ITU-T grid. In addition, serving a connection request that requires b codewords is done by finding any b free codewords and thus simplify the routing and code assignment process and improve the network performance in terms of blocking probability. A further advantage of multicode OCDM is its ability to provide high data rates easily by increasing the number of assigned codes.

However, the use of OCDM poses some limitations. One of the limitations of OCDM is the poor spectral efficiency. In addition, if a user requests b codewords, b encoders/decoders are required in a multicode OCDM network which results in increasing the complexity [8]. Recently, considerable research on improving the spectral efficiency of OCDM systems has been addressed [9]–[12]. In [9], OCDM system with spectral efficiency of 0.125 bit/s/Hz has been demonstrated based on the phase coding of tightly spaced phase-locked laser lines. In [10], Wang *et al.* have successfully demonstrated a cost-effective asynchronous WDM/differential phase shift keying

Manuscript received July 20, 2015; revised October 31, 2015 and December 23, 2015; accepted December 24, 2015. Date of publication December 29, 2015; date of current version February 12, 2016. This work was supported by the Egyptian Ministry of Higher Education. The associate editor coordinating the review of this paper and approving it for publication was W. C. Kwong.

A. E. A. Farghal is with the Department of Electronics and Communications Engineering, Egypt-Japan University of Science and Technology (E-JUST), Alexandria 21934, Egypt (e-mail: ahmed.farghal@ejust.edu.eg).

H. M. H. Shalaby is with the Department of Electronics and Communications Engineering, Egypt-Japan University of Science and Technology (E-JUST), Alexandria 21934, Egypt, on leave from the Department of Electrical Engineering, Alexandria University, Alexandria 21544, Egypt (e-mail: shalaby@ieee.org).

K. Kato and R. K. Pokharel are with the Graduate School of Information Science and Electrical Engineering, Kyushu University, Fukuoka 819-0395, Japan (e-mail: kato@ed.kyushu-u.ac.jp; pokharel@ed.kyushu-u.ac.jp).

Color versions of one or more of the figures in this paper are available online at <http://ieeexplore.ieee.org>.

Digital Object Identifier 10.1109/TCOMM.2015.2512922

(DPSK)-OCDM using hybrid encoder/decoder with spectral efficiency of 0.27 bit/s/Hz. Spectral efficiency of 0.5 bit/s/Hz for spectral phase encoded OCDM system has been reported in [11] using DPSK modulation and integrated ring-resonator-based encoders. Using differential quadrature phase-shift keying (DQPSK) modulation and forward error correction (FEC), a spectral phase-encoded OCDM system have achieved 0.87 bit/s/Hz spectral efficiency [12]. On the other hand, multiport OCDM encoder/decoder based on arrayed-waveguide grating (AWG) is able to generate and recognize multiple coherent time-spreading optical codes simultaneously with a single device, which makes it a potential cost-effective device to reduce the number of encoder/decoders [13]. In addition, using optical codes with cyclic wavelength shifts (e.g., shifted carrier-hopping prime codes [14]), it is possible to use the cyclic frequency AWG (CFAWG) as a compact and cost-effective encoder/decoder for incoherent 2D OCDM [15].

The rest of the paper is organized as follows. Section II reviews the related works. In Section III, the proposed system is introduced. An analytical analysis of the proposed system is studied in Section IV, where the BEP is derived taking into account the effects of multiple-access interference (MAI), avalanche photodiode (APD) noise, and thermal noise under Gaussian approximation assumption. Moreover, the blocking probability and degradation probability of the proposed system taking into consideration the user activity are derived in the same section. Numerical results and discussion are provided in Section V. Finally, Section IV concludes the paper.

II. RELATED WORKS

Supporting multimedia services with differential transmission rate and QoS requirements in OCDM networks has been a subject of enormous research. Various approaches have been proposed to support multirate services provision in OCDM networks such as employing codes with different lengths [16], [17], varying the length of optical frequency hopping patterns [18], and adopting code-shift keying schemes with different number of bits/symbol [19]. A different approach is to use multicode technique, where multirate transmission is achieved by sending different number of distinct codes simultaneously according to user required data rate [8], [20]. Providing time-variant data rates by varying the code length or the length of frequency hopping pattern (according to the changes in the requested bit rate) is not possible since it requires a very complex encoder/decoder structures. Moreover, it is not possible to maintain the auto- and cross-correlation properties between codes. Further, because of the BEP dependence on bit rate (i.e., code length), the several service requirements for bit rate and BEP cannot be easily guaranteed.

On the other hand, variable-weight codes (with identical-chip-power) and multilevel signaling (with different-chip-power) have been introduced to provide QoS differentiation in OCDM networks by controlling the BEP at the receiver [21]–[24]. Moreover, utilizing multilength variable-weight (MLVW) codes [3], [25] and multicode variable-weight (MCVW) codes [8], both multirate and multi-QoS transmission are supported simultaneously. A comparison between using

MCVW codes and MLVW codes is carried out in our previous study [8]. The results show the superiority of using MCVW in terms of BEP, degradation probability, and network throughput.

The authors of [26] have developed a framework for determining the blocking probability and teletraffic capacity in OCDM networks. They used generalized infinite server queue and degradation probability to model the system blocking. Nonetheless, the authors considered only a single-service class system. Moreover, only the MAI is taken into consideration. Using Engset multirate loss model, the blocking probabilities for multiservice class OCDM network adapting MLVW carrier-hopping prime codes are calculated in [3]. Nonetheless, the authors did not consider the effects of user activity and additive noise. In [20], Vardakas *et al.* have proposed a multirate loss model based on a 2D Markov chain for computing the blocking probabilities of an OCDM passive optical network (PON) supporting multirate service classes. They have taken into account the effects of the additive noise and the bursty nature of traffic. However, they have not considered the provision of multi-QoS among the different service classes. Differing from previous works, in this study we tackle supporting time-variant data rates in multi-QoS OCDM networks using multicode technique taking into consideration the user activity and the effects of MAI, APD noise, and thermal noise.

The authors in [25] have suggested two methods for code assignment in a single-code MLVW OCDM network. In the first method, a wavelength is randomly selected among the available wavelengths and one of its unused codes is assigned to the connection, whereas in the second method, an idle code from the wavelength with the least number of active codes is allocated to the connection. In this study, we develop two code assignment strategies, namely, random multicode assignment (RMA) policy and uniform multicode assignment (UMA) policy, taking into account the multiple-codes allocation from the same wavelength group.

The widely used Erlang-loss model and its variants [3], [25] in evaluating the performance of networks with parallel servers are no longer adequate to evaluate the performance of multicode OCDM networks due to ignoring multiple-codes simultaneous allocation and release. On the other hand, multi-dimensional Markov model can obtain the exact state probabilities for networks taking into account the simultaneous resource allocation [1], [2]. However, no closed-form expression to obtain the steady-state probabilities can be derived. Moreover, for large-size networks, which support more service classes and codes, the model will become very complex and time consuming. In this work, we employ the computationally efficient 1D Kaufman-Roberts recursion [27], [28] to estimate the blocking of multicode OCDM network where its accuracy is validated by simulation.

III. SYSTEM MODEL

The proposed system is composed of Q service-classes, where class $j \in \Omega = \{1, 2, \dots, Q\}$ is characterized by its code weight w_j that determines the required QoS. A $(p^k \times L, w = \{w_1, w_2, \dots, w_Q\}, \lambda_a, I)$ fixed-length variable-weight OCFHC/OOCs are employed as 2D signature sequences

with $p^k \geq w_1 > w_2 > \dots > w_Q$. Here p^k denotes the number of available wavelengths per wavelength group, p is a prime number, k is the degree of the primitive polynomial over Galois field $GF(p)$, and L is the code length fixed for all classes. Moreover, λ_a denotes the auto-correlation value and I represents the cross-correlation matrix, defined as:

$$I \stackrel{\text{def}}{=} [I(i, j), \forall i, j \in \Omega], \quad (1)$$

where $I(i, j)$ is the maximum cross-correlation value between the codewords in classes i and j .

The employed OCFHC/OOCs in class $j \in \Omega$ are composed of two codeword groups: C_0 and C_1 . Group C_0 uses one wavelength from the p^k available wavelengths and uses an OOC with cardinality N_j (given by well-known Johnson bound $N_j = \lfloor (L-1)/w_j(w_j-1) \rfloor$) as time-spreading pattern. While in group C_1 , an OCFHC with $p^k(p^k-1)$ different wavelength permutations and N_j OOCs are used as wavelength-hopping and time-spreading patterns, respectively [7]. The number of available codewords in group C_0 and group C_1 in class j will be

$$N_{C_0}^j = p^k N_j, \quad \text{and} \quad [c]N_{C_1}^j = p^k(p^k-1)N_j, \quad (2)$$

respectively, where N_j is subject to the constraint [29]

$$\frac{\sum_{j=1}^Q N_j w_j (w_j - 1)}{L - 1} \leq 1, \quad (3)$$

to ensure that codewords of different code weights have a cross-correlation value bounded by unity. Then, the total cardinality per class j is given by

$$N_c(j) = N_{C_0}^j + N_{C_1}^j = (p^k)^2 N_j. \quad (4)$$

In the proposed multi-QoS multicode OCDM network with time-variant traffic, class j with code weight w_j can be treated as F_j sub-classes with the same QoS, where sub-class $i \in \{1, 2, \dots, F_j\}$ requests i simultaneous codes. Here F_j represents the maximum number of codes that can be assigned to class j connection requests. The number of codes requested by class j sub-classes is assumed to be uniformly distributed among the set $n_j \stackrel{\text{def}}{=} \{1, 2, \dots, F_j\}$, with a probability mass function (pmf) $n_{j,i}$ ($i = 1, 2, \dots, F_j$) such that $\sum_{i=1}^{F_j} n_{j,i} = 1$. Thus, the average number of codes required by connections in class j is given by:

$$\bar{F}_j = \sum_{i=1}^{F_j} i n_{j,i} \quad (5)$$

Equivalently, class j can support $K_j = N_c(j)/\lceil \bar{F}_j \rceil$ active users in each wavelength group in average. Consequently, the total number of active codes per wavelength group in all classes is given by:

$$\mathcal{K} = \sum_{j=1}^Q \lceil \bar{F}_j \rceil K_j. \quad (6)$$

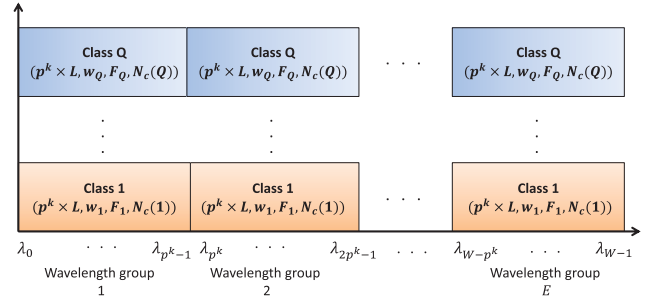


Fig. 1. Fiber bandwidth partitioning in a Q service-class with W wavelengths divided into E wavelength groups.

A. Optical Code Assignment Policies

We consider a single-fiber link with W wavelengths divided into E wavelength groups. Each wavelength group contains p^k wavelengths used for wavelength hopping patterns (see Fig. 1). To provide Q service-class, the available codewords in each wavelength group are divided into Q different code set each with code weight w_j and $N_c(j)$, $j \in \Omega$ available codewords. Based on the required QoS, each code set is assigned to a service-class. The total number of available codewords in class j is

$$\mathcal{L}(j) = E \times N_c(j). \quad (7)$$

The probability density function (pdf) of the occupied codes in each wavelength group depends on the employed code allocation strategy and the offered load. Two code allocation policies are considered in this paper: RMA policy and UMA policy with the restriction that the assigned multiple-codes must be on the same wavelength group.

1) *Random Multicode Assignment (RMA) Policy*: RMA policy arbitrarily chooses wavelength group and allocates i of its ideal codes to the arrived connection request of sub-class i in class j . However, such a multicode assignment method results in a different number of occupied codes in various wavelength groups. Using $\lceil \bar{F}_j \rceil$ as the average number of required codes per class j and assuming that $N_c(j)$ is a multiple of $\lceil \bar{F}_j \rceil$, the pdf of the number of active codes m in a given wavelength group in class j if the number of active codes in a fiber (with E wavelength group) is n can be evaluated from our previous work [8] as:

$$P_M^{(R,j)}(m|n) = \frac{\binom{N_c(j)}{m} \sum_{\mathbf{r} \in \mathcal{R}(j)} \prod_{i=1}^{E-1} \binom{N_c(j)}{r_i \lceil \bar{F}_j \rceil}}{\sum_{\mathbf{n} \in \mathcal{N}(j)} \prod_{i=1}^E \binom{N_c(j)}{n_i \lceil \bar{F}_j \rceil}}, \quad (8)$$

where the two sets $\mathcal{R}(j)$ and $\mathcal{N}(j)$ for class j are defined as:

$$\mathcal{R}(j) \stackrel{\text{def}}{=} \left\{ \mathbf{r} = [r_1, r_2, \dots, r_{E-1}] : \sum_{k=1}^{E-1} r_k = \frac{n-m}{\lceil \bar{F}_j \rceil} \text{ and} \right. \\ \left. r_k \in \left\{ 0, 1, \dots, \frac{N_c(j)}{\lceil \bar{F}_j \rceil} \right\} \forall k \in \{1, \dots, E-1\} \right\}, \quad (9)$$

$$\mathcal{N}(j) \stackrel{\text{def}}{=} \left\{ \mathbf{n} = [n_1, n_2, \dots, n_E]: \sum_{l=1}^E n_l = \frac{n}{\lceil \bar{F}_j \rceil} \text{ and } n_l \in \left\{ 0, 1, \dots, \frac{N_c(j)}{\lceil \bar{F}_j \rceil} \right\} \forall l \in \{1, \dots, E\} \right\}.$$

where n_l is the number of active users (each assigned $\lceil \bar{F}_j \rceil$ codes) in wavelength group $l \in \{1, 2, \dots, E\}$ and r_k is the number of active users (each assigned $\lceil \bar{F}_j \rceil$ codes) in wavelength group $k \in \{1, 2, \dots, E-1\}$. Then, $P_M^{(R,j)}(m)$ is formulated as:

$$P_M^{(R,j)}(m) = \sum_{n=m}^{\mathcal{L}(j)} P_M^{(R,j)}(m|n) P_N^{(j)}(n), \quad (10)$$

where $P_N^{(j)}(n)$ is the probability of the network being in state n for class j . It should be noted that (8) is the hypergeometric distribution modified to account for simultaneously assigning $\lceil \bar{F}_j \rceil$ codes from the same wavelength group to the incoming class j connection requests.

2) *Uniform Multicode Assignment (UMA) Policy*: In UMA policy, a wavelength group with the least number of active codes among other wavelength groups is chosen and $\lceil \bar{F}_j \rceil$ of its unused codes in average are allocated simultaneously to the received connection request of class j . This uniform connection assignment tries to uniformly distribute active codes among different wavelength groups; as a result, QoS in each wavelength group is the same. The amount of resources demanded by class j user connection request can be treated as a user demanding a basic code unit (BCU) that is consisting of $\lceil \bar{F}_j \rceil$ codes. Hence, in each wavelength group there are $H_j = N_c(j)/\lceil \bar{F}_j \rceil$ BCUs for class j .

Algorithm 1 shows the pseudocode of the proposed UMA policy, where $\mathcal{J} \in \{1, 2, \dots, E\}$ is the set of wavelength groups and $C_{h,i}$ is the cost of wavelength group $i \in \mathcal{J}$ in step $h \in \{1, 2, \dots, H_j\}$ in terms of the number of occupied codes. Fig. 2 provides an example of UMA policy. At first all the costs $C_{h,i}$ are initialized to zero. At step (1,1), wavelength group 2 is arbitrary selected and its cost is incremented. At step (1,2), wavelength groups 1 and 3 have the lowest cost, and one of them is arbitrary selected. At step (1,3), only wavelength group 3 has the lowest cost, so it should be selected. At the end of step 1 all wavelength groups have the same number of active codes. In UMA policy, $P_M^{(U,j)}(m)$ is modified from [25] to account for simultaneously allocating $\lceil \bar{F}_j \rceil$ codes to each incoming request in class j in the same wavelength group as follows:

$$P_M^{(U,j)}(m) = \sum_{n=m}^{\mathcal{L}(j)} P_M^{(U,j)}(m|n) P_N^{(j)}(n), \quad (11)$$

where

$$P_M^{(U,j)}(m|n) = \begin{cases} \frac{\text{mod}(n, E\lceil \bar{F}_j \rceil)}{E\lceil \bar{F}_j \rceil}, & m = \lceil \bar{F}_j \rceil \left(\left\lfloor \frac{n}{E\lceil \bar{F}_j \rceil} \right\rfloor + 1 \right) \\ \frac{E\lceil \bar{F}_j \rceil - \text{mod}(n, E\lceil \bar{F}_j \rceil)}{E\lceil \bar{F}_j \rceil}, & m = \lceil \bar{F}_j \rceil \left\lfloor \frac{n}{E\lceil \bar{F}_j \rceil} \right\rfloor \end{cases} \quad (12)$$

and $\text{mod}(x, y)$ represents the remainder of x/y .

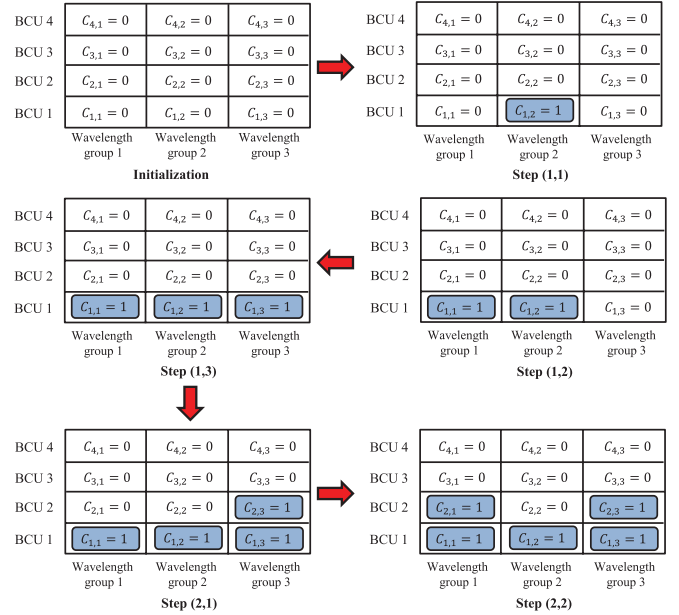


Fig. 2. Example of UMA mechanism for a service-class with BCU that contains $\lceil \bar{F}_j \rceil$ codes in average.

Algorithm 1. Uniform Multicode Assignment Policy

Input : Connection request $\{\lceil \bar{F}_j \rceil, \text{QoS}\}$, number of wavelength groups E , number of class j BCUs H_j

Output: Select wavelength group to serve the request

Initialization:

for $h \leftarrow 1$ **to** H_j **do**

for $i \leftarrow 1$ **to** E **do**

$C_{h,i} \leftarrow 0$

end

end

for $h \leftarrow 1$ **to** H_j **do**

for $i \leftarrow 1$ **to** E **do**

$\mathcal{J}' \leftarrow \{i \in \mathcal{J} | C_{h,i} = \min_{i \in \mathcal{J}} (\sum_{l=1}^h C_{l,i})\}$

 Select arbitrary $i \in \mathcal{J}'$

end

 Connection request $\leftarrow i$;

$C_{h,i} \leftarrow C_{h,i} + 1$;

end

return assigned wavelength group

IV. PERFORMANCE METRICS

In this section, the performance of the proposed network is evaluated by means of the following metrics: BEP, degradation probability, and blocking probability.

A. Bit Error Probability (BEP)

In this subsection, the BEP of the proposed system using APD is derived, taking into account the effects of MAI, APD noise, and thermal noise. In our derivation, we assume a bit-asynchronous chip-synchronous system for ease of analysis. In the more realistic chip-asynchronous case, the performance will

be superior to the case of chip-synchronous since the latter provides BEP upper bound [30]. Denote by q_{ij}^0 and q_{ij}^1 , $i, j \in \Omega$, the one-hit probabilities between the desired codeword, originated from group C_0 and group C_1 , respectively, from class i and an interfering codeword from class j . The one-hit probability for multiservice OCDM system can be obtained following a similar technique as used in [7], [22]:

$$\begin{aligned} q_{ij}^0 &= \frac{w_i w_j (p^k N_j - 1)}{2L(N_c(j) - 1)}, \\ q_{ij}^1 &= \frac{w_i w_j p^k N_j - \min(w_i, w_j)}{2L(N_c(j) - 1)}. \end{aligned} \quad (13)$$

The factor 1/2 accounts for equiprobable on-off data-bit transmission. Then, the average probability of obtaining a one interference hit for the desired codeword of weight w_i correlating with an interfering codeword of weight w_j is given by:

$$q_{ij} = \frac{N_{C_0}^j}{N_c(j)} q_{ij}^0 + \frac{N_{C_1}^j}{N_c(j)} q_{ij}^1 = \frac{w_i w_j}{2p^k L} R_{ij}, \quad (14)$$

where R_{ij} is the ratio of the interfering codewords contributing one-hit to the total interfering codewords in class j , given by:

$$R_{ij} = \frac{((p^k)^2 N_j - 1) - (p^k - 1) / \max(w_i, w_j)}{N_c(j) - 1}. \quad (15)$$

In a Q -class multicode OCDM network with \mathcal{K} available codes in a wavelength group, there are $\sum_{j=1, j \neq k}^Q K_j \lceil \bar{F}_j \rceil + K_k \lceil \bar{F}_k \rceil - 1 = \mathcal{K} - 1$ codes that could interfere with the intended user code in the desired class $k \in \Omega$. Conditioning on the event that ℓ_j , $j \neq k$ codes among $K_j \lceil \bar{F}_j \rceil$ probable interfering codes in class j contributing one interference hit on the desired user code in class k (binomial distribution with probability q_{kj}) and the event that ℓ_k codes out of $K_k \lceil \bar{F}_k \rceil - 1$ probable interfering codes in class k could interfere with the intended user code in class k (binomial distribution with probability q_{kk}). Since the users of various classes are independent, we have

$$\begin{aligned} \Pr\{\ell|\mathcal{K}\} &= \binom{K_k \lceil \bar{F}_k \rceil - 1}{\ell_k} q_{kk}^{\ell_k} (1 - q_{kk})^{K_k \lceil \bar{F}_k \rceil - 1 - \ell_k} \\ &\times \prod_{j=1, j \neq k}^Q \binom{K_j \lceil \bar{F}_j \rceil}{\ell_j} q_{kj}^{\ell_j} (1 - q_{kj})^{K_j \lceil \bar{F}_j \rceil - \ell_j} \end{aligned} \quad (16)$$

where the interfering random vector ℓ is defined as

$$\begin{aligned} \ell \stackrel{\text{def}}{=} &\left\{ [\ell_1, \ell_2, \dots, \ell_Q] : \ell_j \in \{0, 1, \dots, K_j \lceil \bar{F}_j \rceil\} \right. \\ &\forall j \in \{1, \dots, k-1, k+1, \dots, Q\}, \\ &\left. \ell_k \in \{0, 1, \dots, K_k \lceil \bar{F}_k \rceil - 1\}, 0 \leq \sum_{q=1}^Q \ell_q \leq \mathcal{K} - 1 \right\}. \end{aligned} \quad (17)$$

The average BEP P_{E_k} of class k users (with code weight w_k and $\lceil \bar{F}_k \rceil$ parallel codes) given \mathcal{K} codes in a multiservice multicode network is given by:

$$\begin{aligned} P_{E_k} &= \sum_{\ell_1=0}^{K_1 \lceil \bar{F}_1 \rceil} \dots \sum_{\ell_k=0}^{K_k \lceil \bar{F}_k \rceil - 1} \dots \sum_{\ell_Q=0}^{K_Q \lceil \bar{F}_Q \rceil} \Pr\{\ell|\mathcal{K}\} \\ &\times \Pr\{\text{a bit error}|\ell, \mathcal{K}\}, \end{aligned} \quad (18)$$

where $\Pr\{\text{a bit error}|\ell, \mathcal{K}\}$ is the conditional probability of error given the interference vector ℓ and \mathcal{K} codes. Assume that users transmit data bits "0" and "1" with equal probability (i.e., $\Pr\{0\} = \Pr\{1\} = 1/2$). Moreover, denote by Y_k the photon count collected in one bit interval in class k . Given a threshold θ_k , the correlation receiver with hardlimiters declares "1" if $Y_k > \theta_k$ and declares "0" otherwise. The optimum receiver uses the value of θ_k that minimizes the BEP:

$$\begin{aligned} \Pr\{\text{a bit error}|\ell, \mathcal{K}\} &= \frac{1}{2} \min_{\theta_k} (\Pr\{Y_k \leq \theta_k|1, \ell\} + \Pr\{Y_k > \theta_k|0, \ell\}). \end{aligned} \quad (19)$$

Under continuous Gaussian assumption for the photon count Y_k [31], we have

$$\Pr\{Y_k \leq \theta_k|1, \ell\} = Q\left(\frac{\mu_{1k} - \theta_k}{\sigma_{1k}}\right), \quad (20)$$

and

$$\begin{aligned} \Pr\{Y_k > \theta_k|0, \ell\} &= \Pr\{Y_k > \theta_k|0, \ell, Z_k = w_k\} \Pr\{Z_k = w_k\} \\ &\quad + \Pr\{Y_k > \theta_k|0, \ell, Z_k \neq w_k\} \Pr\{Z_k \neq w_k\} \\ &= Q\left(\frac{\theta_k - \mu'_{0k}}{\sigma'_{0k}}\right) \Pr\{Z_k = w_k\} \\ &\quad + Q\left(\frac{\theta_k - \mu_{0k}}{\sigma_{0k}}\right) \Pr\{Z_k \neq w_k\}, \end{aligned} \quad (21)$$

where $Q(x) \stackrel{\text{def}}{=} (1/\sqrt{2\pi}) \int_x^\infty e^{-y^2/2} dy$ and $Z_k \in \{0, 1, \dots, w_k\}$ denotes the number of interfered mark positions in the bit interval of the desired class k user directly after the first optical hardlimiter. The probability distribution of Z_k is adapted here from [32]:

$$\begin{aligned} \Pr\{Z_k = w_k\} &= \Pr\{\alpha_1 \geq 1, \alpha_2 \geq 1, \dots, \alpha_{w_k} \geq 1\} \\ &= \frac{1}{w_k^{\ell_1 + \dots + \ell_Q}} \sum_{t=0}^{w_k-1} (-1)^t \binom{w_k}{t} (w_k - t)^{\ell_1 + \dots + \ell_Q}, \end{aligned} \quad (22)$$

where α_t , $t \in \chi_k \stackrel{\text{def}}{=} \{1, 2, \dots, w_k\}$, denotes the number of interfering hits occurred in the t th marked chip of the desired class k user. It is worthwhile noting that

$$\Pr\{Z_k \neq w_k\} = 1 - \Pr\{Z_k = w_k\}. \quad (23)$$

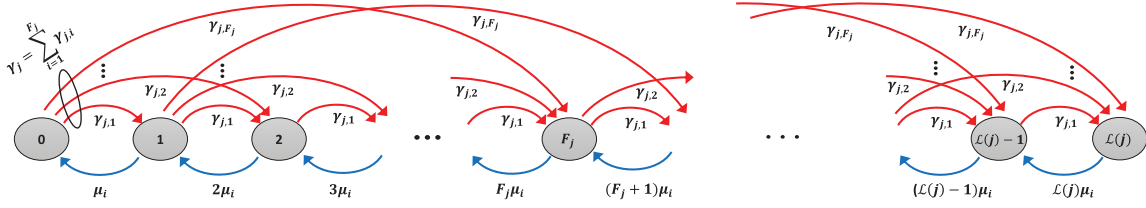


Fig. 3. 1D state-transition diagram for class j with F_j sub-classes.

The expressions for the parameters μ_{0k} , σ_{0k}^2 , μ_{1k} , σ_{1k}^2 , μ'_{0k} and $\sigma_{0k}^{\prime 2}$ for 2D OCFHC/OOC codes are adapted here from [33]:

$$\begin{aligned} \mu_{0k} &= \langle G \rangle n_d, & \sigma_{0k}^2 &= \langle G \rangle^2 F n_d + \sigma_j^2, \\ \mu_{1k} &= \langle G \rangle \left(\sum_{j=1}^{w_k} n_j^k + n_d \right) = \mu'_{0k}, \\ \sigma_{1k}^2 &= \langle G \rangle^2 F \left(\sum_{j=1}^{w_k} n_j^k + n_d \right) + \sigma_j^2 = \sigma_{0k}^{\prime 2}, \end{aligned} \quad (24)$$

where $\langle \cdot \rangle$ represents ensemble averaging, G denotes the stochastic APD gain and n_j^k is the average number of absorbed photons per received single class k user chip, given by:

$$n_j^k = \frac{\eta_j \lambda_j P_c T_c}{hC}, \quad (25)$$

where λ_j is the j th laser wavelength utilized in the code construction, η_j denotes the quantum efficiency at wavelength λ_j , P_c is the received peak laser power per chip, $C = 3 \times 10^8$ m/s is the vacuum speed of light, and $h = 6.626 \times 10^{-34}$ J.s is Plank's constant. $F = \langle G^2 \rangle / \langle G \rangle^2 = k_{\text{eff}} \langle G \rangle + (1 - k_{\text{eff}}) [2 - (1/\langle G \rangle)]$ is the APD excess noise factor, where k_{eff} is the APD effective ionization ratio [34]. While, $n_d = I_d T_c / e$ stands for the average number of dark carriers generated within a chip duration T_c , where I_d is the APD dark current, and $e = 1.6 \times 10^{-19}$ C is the electron charge. $\sigma_j^2 = 2k_B T_n T_c / e^2 R_L$ represents the thermal noise variance within a chip interval, where $k_B = 1.38 \times 10^{-23}$ J/K is Boltzmann's constant, T_n is the receiver noise temperature, and R_L is the receiver load resistance. The BEP minimization problem in (19) is achieved at a decision threshold $\theta_k = (\mu_{0k} \sigma_{1k} + \mu_{1k} \sigma_{0k}) / (\sigma_{0k} + \sigma_{1k})$ [35]. After simple algebraic manipulations, P_{E_k} can be written as:

$$\begin{aligned} P_{E_k} &= \sum_{\ell_1=0}^{K_1 \lceil \bar{F}_1 \rceil} \dots \sum_{\ell_k=0}^{K_k \lceil \bar{F}_k \rceil - 1} \dots \sum_{\ell_Q=0}^{K_Q \lceil \bar{F}_Q \rceil} \\ &\times \binom{K_k \lceil \bar{F}_k \rceil - 1}{\ell_k} q_{kk}^{\ell_k} (1 - q_{kk})^{K_k \lceil \bar{F}_k \rceil - 1 - \ell_k} \\ &\times \prod_{j=1, j \neq k}^Q \binom{K_j \lceil \bar{F}_j \rceil}{\ell_j} q_{kj}^{\ell_j} (1 - q_{kj})^{K_j \lceil \bar{F}_j \rceil - \ell_j} \\ &\times \left[\frac{1}{2} \Pr\{Z_k = w_k\} + Q \left(\frac{\mu_{1k} - \mu_{0k}}{\sigma_{1k} + \sigma_{0k}} \right) \Pr\{Z_k \neq w_k\} \right] \end{aligned} \quad (26)$$

B. Blocking Probability

Fiber links in the proposed system operate as Q independent service-classes, Fig. 1. The users of class $j \in \Omega$ are divided into F_j sub-classes where a sub-class i ($i = 1, \dots, F_j$) user requires i simultaneous codes uniformly distributed on $[1, F_j]$. Moreover, serving a connection request requiring i codewords is done by finding any free i codewords. As only the number of idle codes affects the blocking probability in the proposed multicode OCDM network (codes are identical in contrast to spectrum slots), class $j \in \Omega$ can be modeled as multirate loss queues (MRLQs) with teletraffic capacity of $\mathcal{L}(j)$ codes (servers) shared by F_j sub-classes with using 1D Kaufman-Roberts recursion to obtain the steady-state probabilities of the active codes [27], [28].

We assume that the requested codes of a connection follow a birth-death Markovian model with Poisson arrival process with arrival rate $\gamma_{j,i}$ per time unit for sub-class i connection request in class j and exponentially distributed service time with mean $1/\mu_i$. Thus, the offered traffic load for sub-class i connection is $A_{j,i} = \gamma_{j,i}/\mu_i$, which is assumed to be equal for all sub-classes. Since the requests follow the Poisson process, then the total offered traffic to class j is also Poissonian with total arrival rate $\gamma_j = \sum_{i=1}^{F_j} \gamma_{j,i}$, Fig. 3. In Fig. 3, a transition from state $(n - i)$ to state (n) is due to a new arrival of sub-class i request with arrival rate γ_i and the allocation of i free codes, while transition from state (n) to state $(n - i)$ is due to a completion of sub-class i service (i.e., releasing i codes) with rate $i\mu_i$, where n is the total number of active codes in class j . The steady-state probability $P_N^{(j)}(n)$ of being in state n can be calculated using 1D Kaufman-Roberts recursion [27], [28] as follows:

$$P_N^{(j)}(n) = \frac{\tilde{P}_N^{(j)}(n)}{\sum_{k=0}^{\mathcal{L}(j)} \tilde{P}_N^{(j)}(k)}, \quad (27)$$

where

$$\tilde{P}_N^{(j)}(n) = \begin{cases} 0, & n < 0 \\ 1, & n = 0 \\ \sum_{i=1}^{F_j} \frac{i A_{j,i}}{n} \tilde{P}_N^{(j)}(n - i), & 1 < n \leq \mathcal{L}(j) \end{cases} \quad (28)$$

Blocking happens when a connection request of sub-class i cannot find i free codes (servers). Therefore, the blocking probability $P_{B,i}^{(j)}$ of sub-class i can be found by summing up the probabilities of all states with code occupancies larger than $\mathcal{L}(j) - i$ (i.e., requested bit rate cannot be satisfied):

$$P_{B,i}^{(j)} = \sum_{n=\mathcal{L}(j)-i+1}^{\mathcal{L}(j)} P_N^{(j)}(n), \quad \forall i \leq F_j \quad (29)$$

and the single-link average blocking probability of class j is given by:

$$P_B^{(j)} = \frac{\sum_{i=1}^{F_j} P_{B,i}^{(j)}}{F_j}. \quad (30)$$

Requests for additional codes for an existing connection can be absorbed by allocating a number of unused encoders/decoders corresponding to the required expansion in the transmission rate. These requests can be treated as a new connections generated according to a Poisson process. As before, blocking will happen when the number of requested codes cannot be satisfied.

To successfully establish a lightpath for sub-class i in a multi-code OCDM network, each fiber link traversed by this lightpath should have at least free i codes. Let $P_{B,i(l)}^{(j)}$ denote the blocking probability of sub-class i at the l th link in class j and for simplicity assume traffic independency among the links. Then, the *end-to-end* blocking probability of sub-class i lightpath request is evaluated as

$$P_{B,i_e-e}^{(j)} = 1 - \prod_{H:l \in H} [1 - P_{B,i(l)}^{(j)}] = 1 - [1 - P_{B,i}^{(j)}]^H \quad (31)$$

where $H, H : l \in H$ is the set of links (hops) traversed by the lightpath and the average *end-to-end* blocking probability assuming uniform traffic for sub-classes is $P_{B_e-e}^{(j)} = \sum_{i=1}^{F_j} P_{B,i_e-e}^{(j)} / F_j$.

C. Degradation Probability

The performance of an OCDM network is MAI-limited and depends on the number of simultaneously active users. As a result, if the number of active class j users in a wavelength group exceeds a specified threshold $\Gamma_{Th}^{(j)}$, which represents the maximum number of users (each with $\lceil \bar{F}_j \rceil$ codes in average) that may be simultaneously active in each wavelength group on the network for a given BEP threshold, the desired QoS would be drastically degraded. Therefore, the degradation occurs with probability [8]:

$$\begin{aligned} P_{deg} &= \Pr \left\{ x^{(j)} > \lceil \bar{F}_j \rceil \Gamma_{Th}^{(j)}, \text{ some } j \in \Omega \right\} \\ &= 1 - \Pr \left\{ x^{(j)} \leq \lceil \bar{F}_j \rceil \Gamma_{Th}^{(j)}, \forall j \in \Omega \right\} \\ &= 1 - \prod_{j=1}^Q \left(\sum_{x^{(j)}=0}^{\lceil \bar{F}_j \rceil \Gamma_{Th}^{(j)}} \left[\sum_{m=x^{(j)}}^{N_c(j)} \binom{m}{x^{(j)}} \right. \right. \\ &\quad \left. \left. \times \rho^{x^{(j)}} (1 - \rho)^{m-x^{(j)}} P_M^{(j)}(m) \right] \right). \quad (32) \end{aligned}$$

where $x^{(j)}$ is the number of simultaneously active class j codes in a wavelength group that create interference and ρ represents the probability that a connection transmits data (activity coefficient), which is assumed to be the same for all classes. It is worthwhile pointing out that $P_M^{(j)}(m)$ is given by (10) for RMA

policy and by (11) for UMA policy. For an OCDM network with perfect service availability (i.e., $P_{deg} = 0$) for any offered load, it follows that no more than $\Gamma_{Th}^{(j)}$ (i.e., $\lceil \bar{F}_j \rceil \Gamma_{Th}^{(j)}$ active codes) connections can be accepted in the network. This can be done through defining a blocking threshold $\Lambda_{Th}^{(j)} = \lceil \bar{F}_j \rceil \Gamma_{Th}^{(j)}$ that determines the upper bound of the number of active codes per wavelength group for class j such that the BEP is below a specified threshold. In this case, the blocking probability for sub-class i is called BEP blocking and occurs when the network have enough free codes, but the BEP is above the specified threshold and is given by:

$$P_{B,i}^{(j)} = \sum_{x^{(j)}=E \times \Lambda_{Th}^{(j)} - b_i + 1}^{E \times \Lambda_{Th}^{(j)}} P_N^{(j)}(x^{(j)}). \quad (33)$$

At a specified BEP level in asynchronous OCDM, there is always a set of unused codes. Thus, the network teletraffic capacity (in terms of the number of admitted users for a pre-defined maximum degradation probability [26]) can be relaxed using these unused codes by allowing QoS degradation in terms of BEP to occur with some small probability. This can be done by increasing the number of admitted class j users over $\Gamma_{Th}^{(j)}$, i.e., $\Lambda_{Th}^{(j)} \in \{\lceil \bar{F}_j \rceil \Gamma_{Th}^{(j)}, \lceil \bar{F}_j \rceil \Gamma_{Th}^{(j)} + 1, \dots, N_c(j)\}$. Call admission control algorithms provide means to prevent excessive QoS degradation by checking the interference level caused by the incoming request to decide whether it is accepted or blocked [8], [25], [26].

V. NUMERICAL RESULTS

In this section, we numerically present the performance evaluation results of the proposed multicode OCDM network with time-varying bit rates and QoS differentiation. We consider a two-QoS class network (i.e., $Q = 2$), namely, high QoS (class 1) and low QoS (class 2). The basic bit rate R_b is chosen to be 0.5 Gb/s. The code length is determined by the bit rate and the bandwidth of the wavelength in WDM window. For 50 GHz WDM grid (i.e., bandwidth $\Delta f = 50$ GHz), the chip duration is $T_c = 1/\Delta f = 0.02$ ns and the code length, fixed for both classes, is $L = 1/R_b T_c = 100$. The number of wavelengths in each wavelength group is taken to be 8 (i.e., $p^k = 8$). Since $w_2 < w_1 \leq p^k$, we choose $w_1 = p^k = 8$ (high QoS class). Using $N_1 = \lfloor (L - 1)/w_1(w_1 - 1) \rfloor$, the number of available codes used for time spreading in class 1 is $N_1 = 1$. Normally the users asking for low QoS are greater than those requesting high QoS. So, we set the number of codes used for time spreading in class 2 to be twice the number of codes in class 1, i.e., $N_2 = 2$. The code weight of class 2 (low QoS) is chosen so as to satisfy both the Johnson bound and the constraint in (3), i.e., $w_2 = 5$. Then from (4), the total cardinality of class 1 and class 2 are $N_c(1) = 64$ and $N_c(2) = 128$, respectively. The highest number of simultaneous codes that assigned to class 1 and class 2 is assumed to be 8, i.e., $F_1 = F_2 = 8$ (not necessary to be equal). The number of requested codes for class 1 (class 2) is uniformly distributed between 1 and F_1 (F_2). Using (5), we then have the average number of requested codes $\lceil \bar{F}_1 \rceil = \lceil \bar{F}_2 \rceil = 5$

TABLE I
SYSTEM PARAMETERS

Parameter	Symbol	Value
APD responsivity	$\mathfrak{R} = e\eta_j\lambda_j/hc$	0.84 A/W
APD gain	$\langle G \rangle$	100
APD effective ionization ratio	k_{eff}	0.02
APD dark current	I_d	1 nA
Wavelength range of the first wavelength group	$\lambda_j, j \in \{1, \dots, p^k\}$	1550.0–1552.8 nm (0.4 nm spacing)
Receiver noise temperature	T_n	300° K
Receiver load resistance	R_L	50 Ω

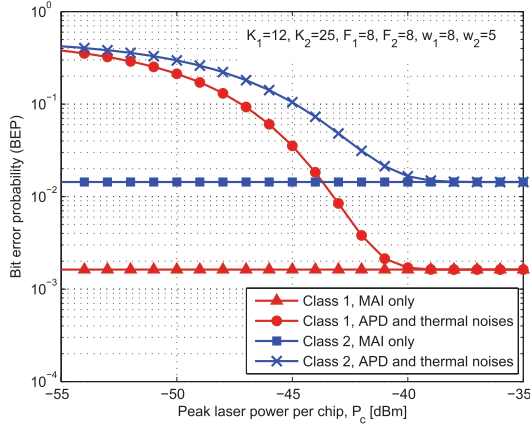


Fig. 4. BEP versus peak laser power per chip, P_c .

corresponding to an average requested bit rate of $\bar{R}_b = 2.5$ Gb/s. Subsequently, the maximum number of users accommodated by class 1 and class 2 are $K_1 \approx 12$ users and $K_2 \approx 25$ users each with 5 codes in average, respectively. The other system parameters used in the numerical evaluation are listed in Table I.

Fig. 4 shows the BEP versus peak laser power per chip P_c for both class 1 and class 2 when $K_1 = 12$ and $K_2 = 25$ users. The BEP of class 2 is worse due to its lower code weight ($w_2 < w_1$). The effects of APD and thermal noises dominate the BEP in the range of small peak laser power per chip. By increasing P_c , the effects of APD and thermal noises are compensated and the system becomes MAI-limited.

Fig. 5 plots the BEP versus the number of simultaneous users in class 1. The number of users in class 2 is kept fixed at $K_2 = 10$. We set the peak laser power per chip $P_c = -37$ dBm, in which the effect of MAI is a dominant source of bit error compared to the effects of APD noise and thermal noise. The figure indicates that class 1 has a degradation threshold $\Gamma_{\text{Th}}^{(1)} = 7$ (i.e., $\lceil \bar{F}_1 \rceil \Gamma_{\text{Th}}^{(1)} = 35$ codes) for which maximum BEP $\leq 10^{-5}$ and class 2 has a degradation threshold $\Gamma_{\text{Th}}^{(2)} = 10$ (i.e., $\lceil \bar{F}_2 \rceil \Gamma_{\text{Th}}^{(2)} = 50$ codes) for for which maximum BEP $\leq 10^{-3}$. The number of simultaneous users can be improved greatly by implementing FEC [33].

Fig. 6 presents the blocking probability of class 1 as a function of the offered load for a connection asking for additional $b \in \{1, 2, \dots, F_1\}$ codes with $E = 6$ and $\Lambda_{\text{Th}}^{(1)} = 35$ (i.e., 210 available codes). From the figure, connection asking for a large number of codes expansion will experience higher blocking probability than connection asking for a small number of codes expansion.

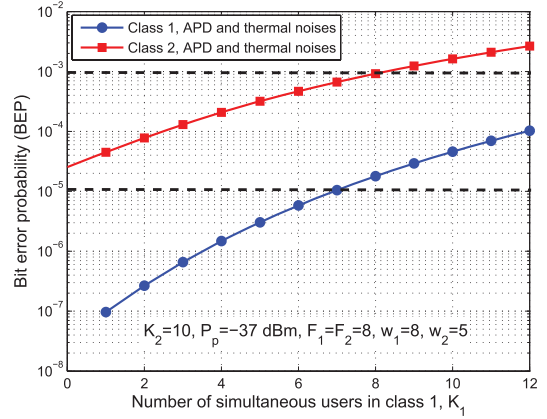


Fig. 5. BEP as a function of the number of class 1 users, K_1 .

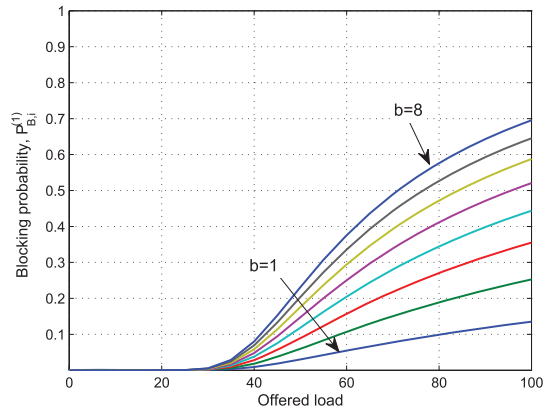


Fig. 6. Class 1 sub-classes blocking probability as a function of the offered load.

Shown in Fig. 7(a) the average *end-to-end* blocking probability for class 1 and class 2 as a function of the offered load per class for $E = 6$. In this figure, considering the obtained $\Gamma_{\text{Th}}^{(i)}$, $i \in \{1, 2\}$ from Fig. 5, the blocking threshold is set to $\Lambda_{\text{Th}}^{(1)} = \Gamma_{\text{Th}}^{(1)} \lceil \bar{F}_1 \rceil = 35$ for class 1 and to $\Lambda_{\text{Th}}^{(2)} = \Gamma_{\text{Th}}^{(2)} \lceil \bar{F}_2 \rceil = 50$ for class 2. From the figure, we observe that class 1 has the worse blocking probability. This is due to the fact that the number of available codes in class 2 are more than class 1, though the QoS of class 1 is better than class 2. Furthermore, RMA and UMA polices have the same blocking probability as only the number of free codes that matters. Fig. 7(b) presents the average *end-to-end* blocking probability as a function of the number of available wavelength groups at an offered load $A = 40$. As expected, the blocking probability decreases as the number of wavelength groups (and hence the number of available codewords) increases. From the figure, it can be seen that the increase of the number of hops traversed by the lightpath increases the *end-to-end* blocking probability.

To validate the accuracy of using Kaufman-Roberts recursion in computing the blocking probability of multicode OCDM network, Fig. 7 also shows the computer simulation results, which match closely with the analytical results for different traffic loads. The simulation was carried out using an event-driven simulator written in MATLAB. Results have been obtained by generating 10^6 connection requests (arrival events) following a Poisson arrival process with exponentially distributed service

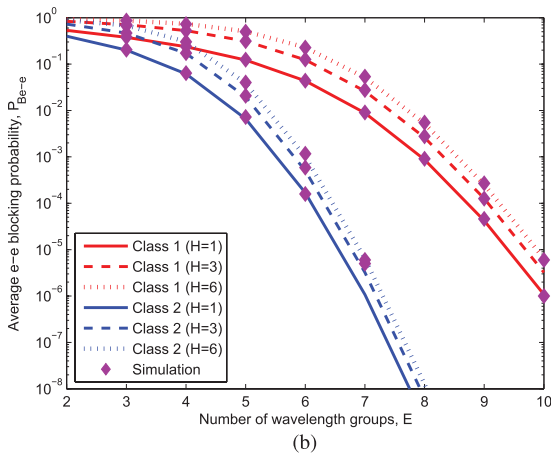
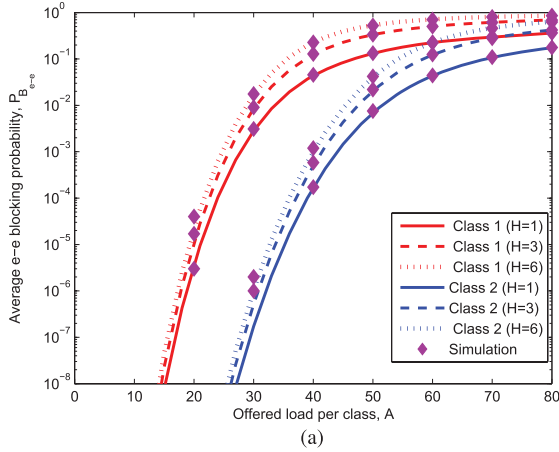


Fig. 7. Average *end-to-end* blocking probability as a function of (a) offered load A , assuming $E = 6$, and (b) number of wavelength groups E , assuming $A = 40$.

times. The number of required codes in class j is uniformly distributed from 1 to F_j with an average $\lceil \bar{F}_j \rceil$ codes.

Next, the relation between the degradation probability P_{deg} and the offered load is investigated with different activity coefficient values in Fig. 8. It is seen that as the activity coefficient increases (i.e., the transmission becomes less bursty) the degradation probability increases. This is owing to the increase in the number of simultaneous active connections which results in increasing the interference level on the network. Additionally, as the offered load increases, the number of connections increases, which consequently results in higher degradation probability. We can also observe that UMA policy has a better performance than that of RMA policy under light traffic offered loads. This is explained by the fact that UMA policy distributes active codes more evenly over all the available wavelength groups, as opposed to RMA policy which distributes active codes randomly among wavelength groups, leading to a different number of occupied codes in various wavelength groups. A wavelength group with more number of connections; its QoS is degraded and the the whole network performance is affected. However, under heavy offered loads, both UMA and RMA policies have the same performance, where all the codes are active.

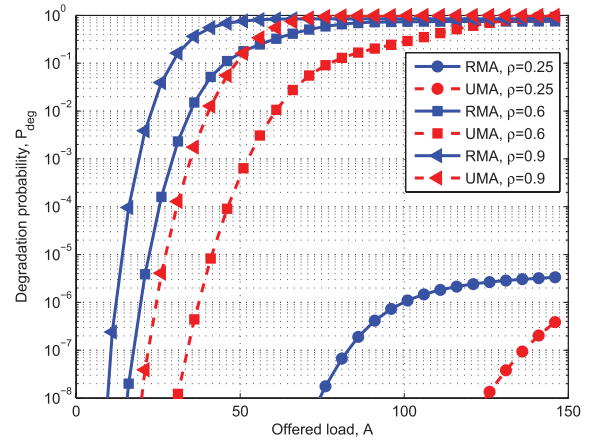


Fig. 8. P_{deg} versus offered load A for different values of the activity coefficient ρ for both RMA and UMA policies.

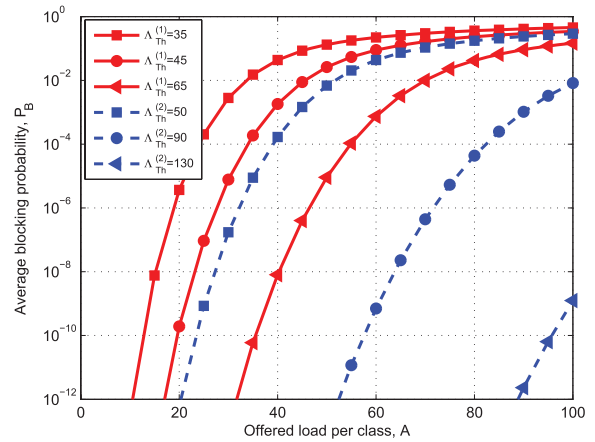


Fig. 9. Average blocking probability as a function of the offered load for different values of the blocking threshold.

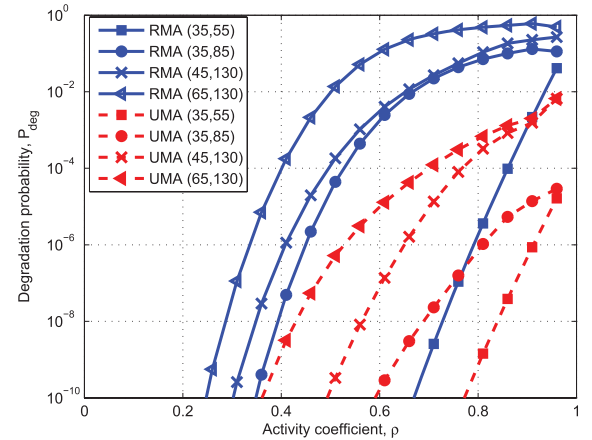


Fig. 10. P_{deg} versus activity coefficient ρ for both RMA and UMA policies with different blocking threshold values.

To show how the network teletraffic capacity can be increased by increasing the blocking threshold, we plot in Fig. 9 the blocking probabilities of both class 1 and class 2 versus the offered load for different threshold values with $E = 6$. It can be shown that increasing $\Lambda_{Th}^{(i)}$, $i \in \{1, 2\}$, leads to a decrease in blocking probability. This is reasonable since increasing $\Lambda_{Th}^{(i)}$ means that more codewords will be available. However,

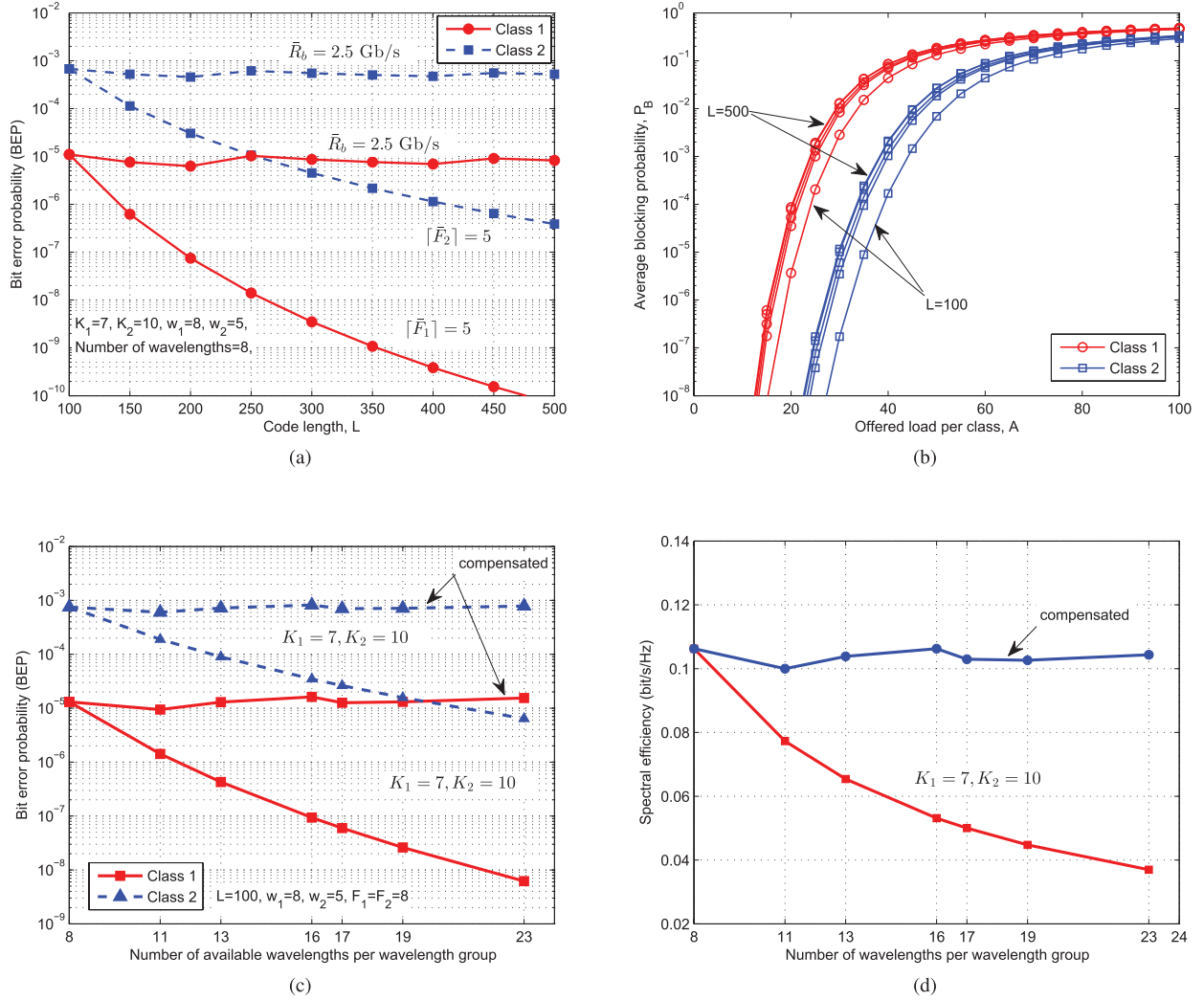


Fig. 11. (a) BEP against the code length, (b) average blocking probability versus offered load for various code length L , (c) BEP versus the number of wavelengths per wavelength group, and (d) spectral efficiency against the number of wavelengths per wavelength group.

this improvement in network teletraffic capacity and blocking probability is paid with an increase in QoS degradation. For a given number of wavelength groups, from Fig. 9, we notice that the blocking probability greatly improves when increasing the blocking threshold rather than increasing the number of wavelength groups as in Fig. 7(b).

The probability of degradation P_{deg} is plotted in Fig. 10 versus the activity coefficient ρ with offered load $A = 50$ for both RMA and UMA policies. In the figure, the numbers in the parentheses represent $\Lambda_{Th}^{(1)}$ and $\Lambda_{Th}^{(2)}$, respectively. It can be seen from the figure that increasing the blocking threshold Λ_{Th} leads to QoS degradation. Moreover, Fig. 10 shows that UMA policy performs better than RMA policy, yielding the lowest probability of QoS degradation. This means that the network teletraffic capacity can be increased greatly using UMA policy with a small degradation probability.

Fig. 11(a) depicts the BEP sensitivity versus the code length L while other parameters are kept fixed. As the code length increases, the possibility of interference decreases, hence that improves the BEP. However, this comes at the expense of decreasing the basic bit rate R_b (and consequently the average

bit rate \bar{R}_b) which is inversely proportional to the code length. Since the number of available codewords is proportional to the code length, it is possible to increase the number of codewords per class and consequently F_j such that each class compensate for the reduction in the average bit rate (i.e. keeping $\bar{R}_b = 2.5$ Gb/s). In this case, it is clear from Fig. 11(a) that the simultaneous increase in L and F_j has no impact on BEP. On the other hand, Fig. 11(b) shows the effect of increasing the code length in combination with increasing F_j on the average blocking probability. It is clear that increasing F_j increases the average blocking probability since a larger number of codes (network resources) are required to meet the user's bit rate. Moreover, increasing F_j will increase the number of encoders/decoders and impose more system complexity. Fig. 11(c) shows the effects of varying the number of available wavelengths per wavelength group on the BEP. The BEP improves with the number of available wavelengths per wavelength group (while all other variables are kept fixed). However, the spectral efficiency will decrease for a fixed number of users as shown in Fig. 11(d). In order to compensate for the spectral efficiency loss, it is required to increase the number of active users by

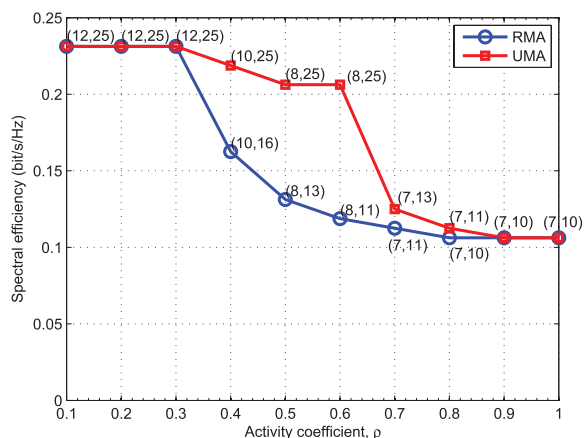


Fig. 12. Spectral efficiency versus activity coefficient for RMA and UMA policies, where $P_{deg}^{max} = 10^{-8}$ and $A = 50$. Numbers in the parentheses indicate the teletraffic capacity of class 1 and class 2, respectively.

the same ratio of increasing the number of wavelengths. From Fig. 11(c), increasing the number of users will cancel out the effect of BEP improvement (BEP is nearly constant). It should be noted that the increment in the number of wavelengths will increase the encoder/decoder complexity with no benefit.

The spectral efficiency for class $j \in \Omega$ is defined as $\eta_j = N_j \bar{R}_b / m \Delta f$, (bit/s/Hz), where $N_j \in \{\Gamma_{Th}^{(j)}, K_j\}$ is the number of simultaneous users in class j for a given BEP and maximum degradation probability P_{deg}^{max} (i.e. teletraffic capacity) and m is the number of wavelengths. In Fig. 12, we compare the achieved total spectral efficiency of multicode OCDM network for RMA policy and UMA policy using call admission control versus the activity coefficient ρ for $P_{deg}^{max} = 10^{-8}$ and offered load $A = 50$. The total spectral efficiency $\eta_t = \sum_{j=1}^Q \eta_j$. From Fig. 12, using UMA policy it is possible to achieve $\eta_t > 0.21$ bit/s/Hz for $\rho \leq 0.6$. However, as the activity coefficient increases, the number of simultaneously active users grows. Thus the blocking threshold should be decreased to satisfy the degradation probability $P_{deg} \leq P_{deg}^{max}$ resulting in decreasing the achieved spectral efficiency.

VI. CONCLUSION

In this paper, we have proposed a multicode OCDM network that has the capability to assign codes elastically according to the data rate requested by connections. In addition, QoS differentiation is achieved by using variable-weight codewords. Two code-assignment policies have been introduced: random multicode assignment (RMA) and uniform multicode assignment (UMA) policies. Several performance measures, namely, BEP, degradation probability, and blocking probability have been evaluated for the proposed network. The effects of APD noise, thermal noise, and MAI have been taken into account in the BEP evaluation. Blocking has been determined by the error probability rather than the exact number of available codes. Our results reveal that the blocking probability and network teletraffic capacity can be improved significantly when employing UMA policy and allowing controllable QoS degradation using call admission control algorithm.

REFERENCES

- [1] G. Zhang, M. D. Leenheer, A. Morea, and B. Mukherjee, "A survey on OFDM-based elastic core optical networking," *IEEE Commun. Surveys Tuts.*, vol. 15, no. 1, pp. 65–87, Feb. 2013.
- [2] H. Beyranvand, M. Maier, and J. A. Salehi, "An analytical framework for the performance evaluation of node- and network-wise operation scenarios in elastic optical networks," *IEEE Trans. Commun.*, vol. 62, no. 5, pp. 1621–1633, May 2014.
- [3] Y. Deng and P. R. Prucnal, "Performance analysis of heterogeneous optical CDMA networks with bursty traffic and variable power control," *IEEE/OSA J. Opt. Commun. Netw.*, vol. 3, no. 6, pp. 487–492, Jun. 2011.
- [4] T. Kodama, N. Wada, G. Cincotti, and K. Kitayama, "Asynchronous OCDM-based 10 G-PON using cascaded multiport E/Ds to suppress MAI noise," *J. Lightw. Technol.*, vol. 31, no. 20, pp. 3258–3266, Oct. 2013.
- [5] S. Huang, K. Baba, M. Murata, and K. Kitayama, "A study on cycle attack by multiaccess interference in multigranularity OCDM-based optical networks," *J. Lightw. Technol.*, vol. 26, no. 14, pp. 2064–2073, Jul. 2008.
- [6] T. Khattab and H. Alnuweiri, "Optical CDMA for all-optical sub-wavelength switching in core GMPLS networks," *IEEE J. Sel. Areas Commun.*, vol. 25, no. 5, pp. 905–921, Jun. 2007.
- [7] S. Shurong, H. Yin, Z. Wang, and A. Xu, "A new family of 2-D optical orthogonal codes and analysis of its performance in optical CDMA access networks," *J. Lightw. Technol.*, vol. 24, no. 4, pp. 1646–1653, Apr. 2006.
- [8] A. E. Farghal, H. M. H. Shalaby, and Z. Kawasaki, "Multirate multiservice all-optical code switched GMPLS core network utilizing multicode variable-weight optical code-division multiplexing," *IEEE/OSA J. Opt. Commun. Netw.*, vol. 6, no. 8, pp. 670–683, Aug. 2014.
- [9] S. Etemad *et al.*, "Spectrally efficient optical CDMA using coherent phase-frequency coding," *IEEE Photon. Technol. Lett.*, vol. 17, no. 4, pp. 929–931, Apr. 2005.
- [10] X. Wang, N. Wada, T. Miyazaki, G. Cincotti, and K. Kitayama, "Field trial of 3-WDM \times 10-OCDMA \times 10.71-Gb/s asynchronous WDM/DPSK-OCDMA using hybrid E/D without FEC and optical thresholding," *J. Lightw. Technol.*, vol. 25, no. 1, pp. 207–215, Jan. 2007.
- [11] A. Agarwal, P. Toliver, T. Banwell, R. Menendez, J. Jackel, and S. Etemad, "Spectrally efficient DPSK-OCDMA coherent system using integrated ring-resonator-based coders," presented at the Opt. Fiber Commun. Conf., Anaheim, CA, USA, Mar. 27–29, 2007, paper OMO5.
- [12] P. Toliver, A. Agarwal, T. Banwell, R. Menendez, J. Jackel, and S. Etemad, "Demonstration of high spectral efficiency coherent OCDM using DQPSK, FEC, and integrated ring resonator-based spectral phase encoder/decoders," presented at the Opt. Fiber Commun. Conf., Anaheim, CA, USA, Mar. 27–29, 2007, PDP7.
- [13] G. Cincotti, N. Wada, and K. Kitayama, "Characterization of a full encoder/decoder in the AWG configuration for code-based photonic routers—Part 1: Modeling and design," *J. Lightw. Technol.*, vol. 24, no. 1, pp. 103–112, Jan. 2006.
- [14] E. Narimanov, W. C. Kwong, G.-C. Yang, and P. R. Prucnal, "Shifted carrier-hopping prime codes for multicode keying in wavelength-time O-CDMA," *IEEE Trans. Commun.*, vol. 53, no. 12, pp. 2150–2156, Dec. 2005.
- [15] J.-F. Huang, C.-C. Yang, and S.-M. Lin, "Realization of one-coincidence wavelength-time coding using extended-quadratic-congruence and optical-orthogonal codes over waveguide-grating optical code-division multiple-access network codes," *Opt. Eng.*, vol. 47, no. 4, pp. 045006-1–045006-10, Apr. 2008.
- [16] W. C. Kwong and G.-C. Yang, "Design of multilength optical orthogonal codes for optical code-division multiple-access multimedia networks," *IEEE Trans. Commun.*, vol. 50, no. 8, pp. 1258–1265, Aug. 2002.
- [17] X. Li and L. Lu, "General construction method of multilength optical orthogonal codes with arbitrary cross-correlation constraint for OCDMA multimedia network," *IEEE/OSA J. Opt. Commun. Netw.*, vol. 7, no. 3, pp. 156–163, Mar. 2014.
- [18] E. Intay, H. M. H. Shalaby, P. Fortier, and L. A. Rusch, "Multirate optical fast frequency-hopping CDMA system using power control," *J. Lightw. Technol.*, vol. 20, no. 2, pp. 166–177, Feb. 2002.
- [19] C.-Y. Chang, G.-C. Yang, and W. C. Kwong, "Wavelength-time codes with maximum cross-correlation function of two for multicode-keying optical CDMA," *J. Lightw. Technol.*, vol. 24, no. 3, pp. 1093–1100, Mar. 2006.
- [20] J. S. Vardakas, I. D. Moscholios, M. D. Logothetis, and V. G. Stylianakis, "Performance analysis of OCDMA PONs supporting multi-rate bursty traffic," *IEEE Trans. Commun.*, vol. 61, no. 8, pp. 3374–3384, Aug. 2013.
- [21] F.-R. Gu and J. Wu, "Construction and performance analysis of variable-weight optical orthogonal codes for asynchronous optical CDMA systems," *J. Lightw. Technol.*, vol. 23, no. 2, pp. 740–748, Feb. 2005.

- [22] W. Liang, H. Yin, L. Qin, Z. Wang, and A. Xu, "A new family of 2D variable-weight optical orthogonal codes for OCDMA systems supporting multiple QoS and analysis of its performance," *Photon. Netw. Commun.*, vol. 16, no. 1, pp. 53–60, Mar. 2008.
- [23] H. Beyranvand and J. A. Salehi, "Application of optical multilevel transmission technique in WDM/OCDM-based core networks," *IEEE Commun. Mag.*, vol. 52, no. 8, pp. 116–125, Aug. 2014.
- [24] H.-H. Yuan, G.-C. Yang, C.-Y. Chang, and W. C. Kwong, "Accurate analysis of double-weight codes with an arbitrary maximum cross-correlation value for two-chip-power optical CDMA," *IEEE Trans. Commun.*, vol. 61, no. 6, pp. 2488–2497, Jun. 2013.
- [25] H. Beyranvand and J. A. Salehi, "Multiservice provisioning and quality of service guarantee in WDM optical code switched GMPDS core network," *J. Lightw. Technol.*, vol. 27, no. 12, pp. 1754–1762, Jun. 2009.
- [26] S. Goldberg and P. Prucnal, "On the teletraffic capacity of optical CDMA," *IEEE Trans. Commun.*, vol. 55, no. 7, pp. 1334–1343, Jul. 2007.
- [27] J. S. Kaufman, "Blocking in a shared resource environment," *IEEE Trans. Commun.*, vol. C-29, no. 10, pp. 1474–1481, Oct. 1981.
- [28] J. W. Roberts, "A service system with heterogeneous user requirements: Application to multi-service telecommunications systems," in *Proc. Perform. Data Commun. Syst. Appl.*, 1981, pp. 423–431.
- [29] N. G. Tarhuni, T. O. Korhonen, E. Mutafungwa, and M. S. Elmusrati, "Multiclass optical orthogonal codes for multiservice optical CDMA networks," *J. Lightw. Technol.*, vol. 24, no. 2, pp. 694–704, Feb. 2006.
- [30] T.-C. Wang, G.-C. Yang, C.-Y. Chang, and W. C. Kwong, "A new family of 2-D codes for fiber-optic CDMA systems with and without the chip-synchronous assumption," *J. Lightw. Technol.*, vol. 27, no. 14, pp. 2612–2620, Jul. 2009.
- [31] R. M. Gagliardi and S. Karp, "Optical digital communications," in *Optical Communications*, 2nd ed. Hoboken, NJ, USA: Wiley, 1995.
- [32] H. Beyranvand, S. A. Nezamalhosseini, J. A. Salehi, and F. Marvasti, "Performance analysis of equal-energy two-level OCDMA system using generalized optical orthogonal codes," *J. Lightw. Technol.*, vol. 31, no. 10, pp. 1573–1584, May 2013.
- [33] A. L. Sanchez, J. V. dos Reis Jr., and B.-H. V. Borges, "Analysis of high-speed optical wavelength/time CDMA networks using pulse-position modulation and forward error correction techniques," *J. Lightw. Technol.*, vol. 27, no. 22, pp. 5134–5144, Nov. 2009.
- [34] J. C. Campbell, "Recent advances in telecommunications avalanche photodiodes," *J. Lightw. Technol.*, vol. 25, no. 1, pp. 109–121, Jan. 2007.
- [35] G. P. Agrawal, *Fiber-Optic Communication Systems*, 3rd ed. Hoboken, NJ, USA: Wiley, 2002, p. 164.



2011. From November 2014 to July 2015, he joined Kyushu University, Fukuoka, Japan, as a Special Research Student. He is currently with the Department of Electronics and Electrical Communications Engineering, Faculty of Electronic Engineering, Menoufiya University, Egypt, where he is an Assistant Professor. His research interests include optical CDMA, all-optical networks (AONs), QoS provisioning in optical networks, elastic optical networking, green optical networks, and nano-optoelectronic devices.



Communications Engineering, School of Electronics, Communications, and

Ahmed E. A. Farghal received the B.Sc. (with Hons.) and M.Sc. degrees from Menoufiya University, Shibin Al Kawm, Egypt, and the Ph.D. degree from Egypt-Japan University for Science and Technology (E-JUST), New Borg EL-Arab City, Alexandria, Egypt, all in electrical engineering, in 2006, 2011, and 2015, respectively. In 2007, he joined the Department of Electronics and Electrical Communications Engineering, Faculty of Electronic Engineering, Menoufiya University, Egypt, and was promoted to the position of a Lecturer Assistant in 2014 to July 2015, he joined Kyushu University, Fukuoka, Japan, as a Special Research Student. He is currently with the Department of Electronics and Electrical Communications Engineering, Faculty of Electronic Engineering, Menoufiya University, Egypt, where he is an Assistant Professor. His research interests include optical CDMA, all-optical networks (AONs), QoS provisioning in optical networks, elastic optical networking, green optical networks, and nano-optoelectronic devices.

Hossam M. H. Shalaby (S'83–M'91–SM'99) was born in Giza, Egypt, in 1961. He received the B.S. and M.S. degrees from Alexandria University, Alexandria, Egypt, and the Ph.D. degree from the University of Maryland, College Park, MD, USA, all in electrical engineering, in 1983, 1986, and 1991, respectively. In 1991, he joined the Department of Electrical Engineering, Alexandria University, and was promoted to Professor in 2001. Currently, he is on leave from Alexandria University, where he is the Chair of the Department of Electronics and

Computer Engineering, Egypt-Japan University of Science and Technology (E-JUST), New Borg EL-Arab City, Alexandria, Egypt. From December 2000 to 2004, he was an Adjunct Professor with the Faculty of Sciences and Engineering, Department of Electrical and Information Engineering, Laval University, Quebec, QC, Canada. From September 1996 to February 2001, he was on leave from the Alexandria University. From September 1996 to January 1998, he was with the Department of Electrical and Computer Engineering, International Islamic University Malaysia, Kuala Lumpur, Malaysia, and from February 1998 to February 2001, he was with the School of Electrical and Electronic Engineering, Nanyang Technological University, Singapore. He has been working as a Consultant with SysDSOFT Company, Alexandria, Egypt, from 2007 to 2010. His research interests include optical communications, silicon photonics, optical space-division multiplexing, optical CDMA, optical OFDM technology, and information theory. He has served as a Student Branch Counselor with Alexandria University, the IEEE Alexandria and North Delta Subsection, from 2002 to 2006, and served as the Chairman of the student activities committee of the IEEE Alexandria Subsection from 1995 to 1996. He was the recipient of an SRC Fellowship from 1987 to 1991 from Systems Research Center, College Park, MD, USA, State Excellence Award in Engineering Sciences in 2007 from Academy of Scientific Research and Technology, Egypt, Shoman Prize for Young Arab Researchers in 2002 from Abdul Hameed Shoman Foundation, Amman, Jordan, State Incentive Award in Engineering Sciences in 1995 and 2001 from Academy of Scientific Research and Technology, Egypt, University Excellence Award in 2009 from Alexandria University, and University Incentive Award in 1996 from Alexandria University.



Kazutoshi Kato (A'91–M'93–SM'12) received the B.S. and M.S. degrees in physics and the Ph.D. degree from Waseda University, Tokyo, Japan, in 1985, 1987, and 1993, respectively. Since 1987, he had been with NTT Opto-Electronics Laboratories, Kanagawa, Japan, where he had been engaged in research on receiver OEICs, high-speed p-i-n PDs and photoreceivers for wide-band transmissions, microwave applications, and optical access networks. From 1994 to 1995, he was on leave from NTT at France Telecom CNET Bagnaux Laboratory, France, as a Visiting Researcher working on MSM PDs. From 2000 to 2003, he was with NTT Electronics Corporation, where he was involved in developing photonic network systems. From 2009 to 2011, he was an Executive Manager with the NTT Photonics Laboratories, Atsugi, Japan. He is currently a Professor of information science and electrical engineering, Kyushu University, Fukuoka, Japan. His research interests include advanced opto-electronics devices and subsystems for high-speed optical transmissions. He is a Senior Member of the Institute of Electronics, Information and Communication Engineers (IEICE), Japan, and a Member of the Japan Society of Applied Physics.



Ramesh K. Pokharel (M'03) received the M.E. and doctorate degrees from the University of Tokyo, Tokyo, Japan, all in electrical engineering, in 2000 and 2003, respectively. He had short academic and industrial experiences in Nepal before he joined the University of Tokyo in 1997, as a Research Student. He had been a Postdoctoral Research Fellow with the Department of Electrical Engineering and Electronics, Aoyama Gakuin University, Tokyo, Japan from April 2003 to March 2005. In April 2005, he joined the Department of Electronics, Graduate School of Information Science and Electrical Engineering, Kyushu University, Fukuoka, Japan, where he is now a Professor. His research interests include low cost RFIC and analog circuits for microwave and millimeter wave wireless communications, on-chip signal integrity issues, and on-chip meta-materials in CMOS. He was the Vice-Director of the Center for Egypt-Japan Co-Operation in Science and Technology of Kyushu University from 2012 to 2013, where he has been serving as the Director since April 2014. He served as the Secretary of the IEEE MTT-S Japan Society from January 2012 to December 2013 and has been serving as the Vice-Chair of education committee of the IEEE-MTT-S Japan Society since January 2014. He was the recipient of the Monbu-Kagakusho Scholarship of the Japanese Government from 1997–2003, and an Excellent COE Research Presentation Award from the University of Tokyo in 2003.